

# Reliability Improvement of Grid Connected PV Inverter Considering Monofacial and Bifacial Panels Using Hybrid IGBT

Srikanth S<sup>1</sup> and Dr. Byamakesh Nayak<sup>2</sup>

<sup>1</sup>Research scholar at School of Electrical Engineering, Kalinga Institute of Industrial Technology, Bhubaneswar, Odisha; srikanth269@gmail.com

<sup>2</sup>Professor and Dean, School of Electrical Engineering, Kalinga Institute of Industrial Technology, Bhubaneswar, Odisha

\*Correspondence: Srikanth S.; srikanth269@gmail.com

**ABSTRACT-** The development of bifacial photovoltaics has led to significant advancements in solar energy. Unlike traditional solar panels, which only generate electricity from the front side, these panels capture the energy from the rear and front surfaces. Bifacial photovoltaics utilize a dual-sided absorption to capture the sunlight that falls on nearby structures and the ground. This technology helps boost their efficiency and makes them an economical and sustainable choice. Furthermore, the increased energy production from the rear side of bifacial panels may lead to higher voltage fluctuations, which affects the thermal stability of PV inverter. Nevertheless, PV inverter is regarded as critical component which affects the reliability performance. Hence in this paper reliability improvement methodology with hybrid IGBT is proposed for the PV inverter. The hybrid IGBT consists of Silicon (Si) IGBT and Silicon Carbide (SiC) Schottky diode. A test case of 3-kW Monofacial and Bifacial grid connected PV inverter system with various albedos is considered. Mission profile for one year at Hyderabad, India location is logged for the assessment. B10 lifetime is calculated for the proposed hybrid IGBT. The effectiveness of the proposed hybrid IGBT is evaluated in comparison with conventional IGBT. The proposed hybrid IGBT significantly improves the reliability performance of the PV inverter.

**Keywords:** IGBT, PV Inverter, Reliability, Silicon (Si), Silicon Carbide (SiC).

## ARTICLE INFORMATION

**Author(s):** Srikanth S and Dr. Byamakesh Nayak;

**Received:** 19/02/2024; **Accepted:** 16/04/2024; **Published:** 30/04/2024;

**e-ISSN:** 2347-470X;

**Paper Id:** IJEER 1902-20;

**Citation:** 10.37391/IJEER.120216

**Webpage-link:**

<https://ijeer.forexjournal.co.in/archive/volume-12/ijeer-120216.html>

**Publisher's Note:** FOREX Publication stays neutral with regard to Jurisdictional claims in Published maps and institutional affiliations.



## 1. INTRODUCTION

The advancement of bifacial photovoltaics (PV) technology has made it possible to harvest more solar energy. Compared to traditional solar panels, which only absorb the sunlight coming from the front side, these bifacial panels capture the sunlight coming from both the rear and front surfaces [1]. The dual-sided absorption of bifacial photovoltaic panels leads to higher energy production and makes them more sustainable. They can be mounted on various types of structures and can be operated in different ways to optimize their energy capture. In areas with high albedo, such as sand or snow, bifacial panels can help improve the energy output of solar systems by capturing the sunlight coming from these surfaces [2]. In order to make them more efficient, ongoing studies are being conducted on how to improve the power flow of these panels. Bifacial photovoltaics technology is playing an important role in meeting the increasing demand for energy from renewable sources [3]. However, the ability to harvest solar energy from both the rare

and front surfaces of the panels can increase the load on the inverters, which effects the reliability performance. Nevertheless, inverter is reported as the critical component in the PV system. To improve the reliability of the power semiconductors, today's research focusses on SiC based power semiconductors.

Due to its exceptional performance in power electronic devices, such as switches, Silicon Carbide has emerged as a promising material. Compared to traditional silicon-based technologies, SiC offers numerous advantages, making it an ideal choice for high-speed applications. Its wide bandgap characteristic enables high breakdown voltages and helps devices operate at elevated temperatures. In [4] proposed a single-channel, voltage-fed AC/DC converter that utilizes a Si IGBT/SiC hybrid switch. By adding two switches at the input side, we were able to reduce the number of devices required. In [5] proposed an improved 4H-SiC IGBT with enhanced modulation that is considered to be 3-D. The suggested IGBT structure is said to be composed of a gate that wraps around a raised channel, which is different from the traditional 2D structure. An optimal design to extract the parameters for the hybrid switch is proposed in [6]. In [7] presented the design of a PV inverter with a low inductance T-type configuration utilizing SiC-MOS, IGBT, and SIIGBT.

In [8] proposed a hybrid modular converter (MMC) topology that features two types of submodules: one of which is based on SiC MOSFET, and the other is based on IGBT. The suggested hybrid configuration can reduce the blocking voltage requirement of the SiC MOSFET by half. In [9] presented a hybrid switch configuration that utilizes two types of IGBT and

two types of SiC hybrid switches. It is said to be very efficient and has low device cost. In [10] implemented a prototype of SiC MOSFET based 4.5-kW DC-AC converter was tested and operated. In [11] presented a hybrid switch that is based on the Si IGBT and the SiC MOSFET technology for DC applications. The proposed SSCB has lower losses than the pure IGBT-based model. In [12] analysed performance of different flow channels and their fluid characteristics to determine the design of a cooling flow fin. This feature was then refined to provide an indication of the hybrid module's heat transfer.

In [13] presented the concept of a hybrid switch that is powered by the combination of a SiC FET and a Si IGBT. The static and dynamic characteristics of the two different hybrid switches are then compared. In [14] presented a novel method for controlling the gate turn-off time of a Si/SiC HyS-based hybrid switch. It is based on a mathematic power loss model. The suggested gate turn-off time can be efficiently achieved across a wide load range. In [15] investigated and compared the effects of the FRV phenomena on the different technologies that are commonly used in the production of Si-IGBTs. It also tests the system level impact of these hybrid devices with the ANPC topology.

In [16] developed a hybrid Si IGBT and SiC MOSFET for Half-bridge 1.7 kV power module. In [17] proposed a power loss model for the ANPC inverter topology, taking into account the modulation strategy and the characteristics of the hybrid switches. In [18] presented a hybrid FC-MMC topology that is powered by the combination of a Si IGBT and a SiC MOSFET.

The converter arms are also equipped with multiple Si SMs. In [19] proposed CTV-ATC method to analyse the issues of thermal variation caused by time variations. In [20] explores the design suitability of the Si IGBT architecture for the given area ratio of the IGBT-MOSFET. Up to 80% of the system's performance can be achieved with the hybrid switch concept. In [21] presented a dual-mode HyS configuration, which features a 1200V 12A SiC MOSFET and a 40A IGBT. The different degradation mechanisms of the system are analysed and studied under the AC power cycle. In [22] presented a high-performance traction converter that uses all-silicon carbide technology. It is designed for use in new light rail systems.

As the SiC is not economical in this paper reliability improvement methodology with hybrid IGBT is proposed for the PV inverter. The hybrid IGBT consists of Silicon (Si) IGBT and Silicon Carbide (SiC) Schottky diode. A test case of 3-kW Monofacial and Bifacial grid connected PV inverter system with various albedos is considered. Mission profile for one year at Hyderabad, India location is logged for the assessment. Foster ETM is used to obtain the junction temperature (JT). JT variations are analysed by using Rainflow (CRF) algorithm. Monte Carlo Simulation (LMCS) is used to produce 10000 populations. B10 lifetime is calculated for the proposed hybrid IGBT. The effectiveness of the proposed hybrid IGBT is evaluated in comparison with conventional IGBT. The proposed hybrid IGBT significantly improves the reliability performance of the PV inverter.

## 2. PROPOSED HYBRID IGBT MODULE

The incorporation of Silicon Carbide technology into power electronic devices represents a paradigm shift in the way power electronics is done. Compared to traditional silicon-based components, these modules offer numerous advantages, such as better efficiency and performance. They integrate various power devices, like Schottky diodes and MOSFETs, into a single package. The high thermal conductivity and wide bandgap of silicon carbide make it an ideal material for power modules [23], [24]. In this paper, hybrid IGBT with Silicon (Si) IGBT and antiparallel Silicon Carbide (SiC) Schottky diode is proposed as shown in *figure. 1*.

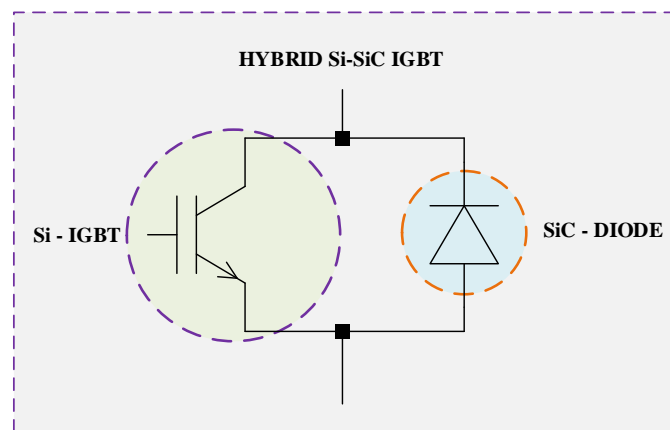


**Figure 1.** Proposed Hybrid IGBT

The thermal models of Si-IGBT and Si-Diode are based on the materials produced by Infineon and Wolf speed respectively. The comparison of properties for Si and SiC materials are presented in *figure. 2*.

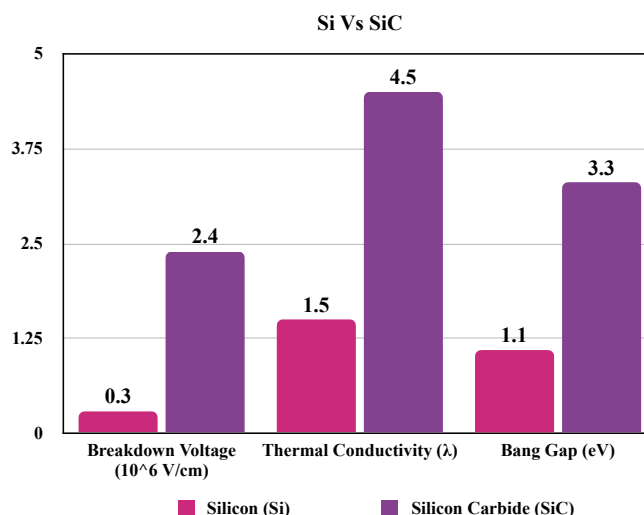


**Figure 2.** Properties Comparison (Si Vs SiC)

### 2.1. Reliability Assessment Methodology

Reliability assessment methodology consists of various stages. To obtain the PV inverter reliability, component level (LC)

reliability is obtained and then system level (LS) is obtained by series reliability block diagram. The flowchart for the reliability assessment is presented in figure 3.

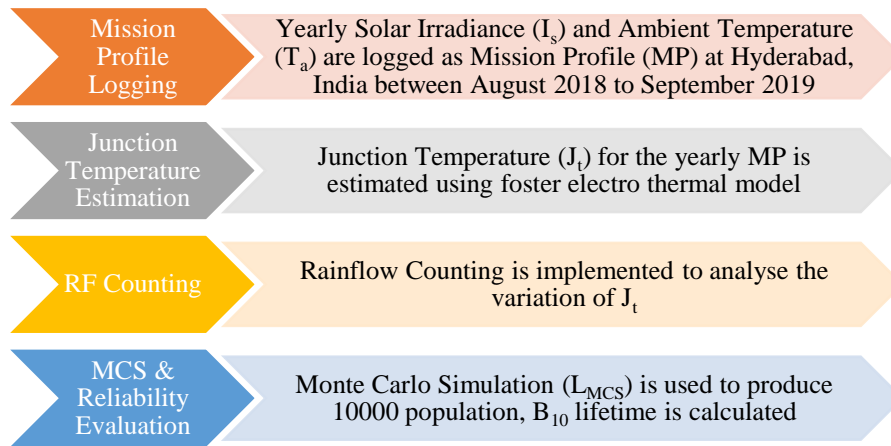


**Figure 3.** Reliability Assessment Flow chart

The  $L_F$  is calculated by using the lifetime equation of the Bayerer as show in equation. 1

$$L_f = \frac{1}{\sum \frac{\text{No.of cycles } (n_i)}{A(\Delta T_j)^{\beta_1} \cdot e^{-(T_j + 273)} \cdot t_{0n} \beta_3 \cdot I \beta_4 \cdot V \beta_5 \cdot D \beta_6}} \quad (1)$$

Monte Carlo Simulation ( $L_{MCS}$ ) is used to produce 10000 population.  $L_F$  at each population is computed using Eq. 1 and fitted in Weibull distribution.  $L_C$  and  $L_S$  reliability are calculated using the equation. 2 and equation. 3 respectively.

$$R_i(t) = e^{-\left(\frac{t}{\alpha}\right)^\gamma} \quad (2)$$

Where

$R_i(t)$  = Reliability of individual component

$\alpha$  = Scale Parameter

$\gamma$  = Shaper Parameter

$$R_{\text{total}}(t) = \prod_{i=1}^n R_i(t) \quad (3)$$

## 2.2. Case Study

A case study of 3-kW Monofacial and Bifacial grid connected PV inverter system is considered as shown in figure. 4. Mission profile for one year with one minute resolution at Hyderabad, India location is logged for the assessment as shown figure. 5. System specifications are tabulated in table 1.

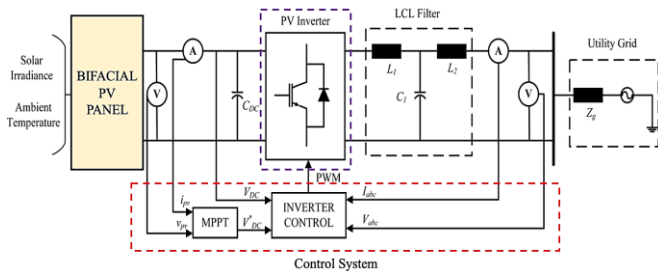


**Figure. 4.** Test Case

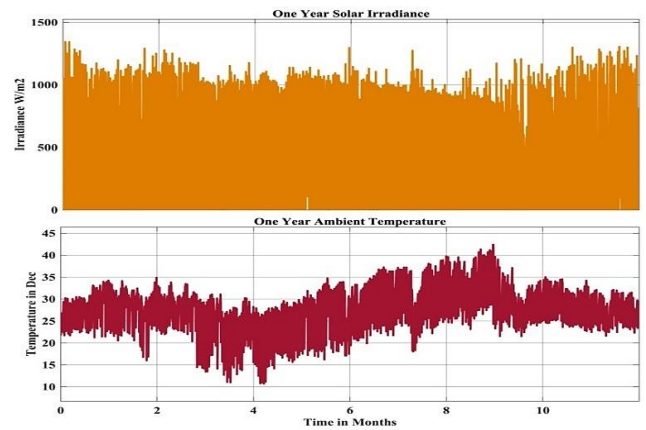


**Figure. 5** Monthly MP for One Year

**Table 1.** System Specifications

Item	Specifications
PV Panel	BP (365)
IGBT	IGW30N60H3
Grid Voltage	230 Volts
Grid Frequency	50 Hz

The bifacial PV panels are modelled under various albedos as shown in figure. 6.

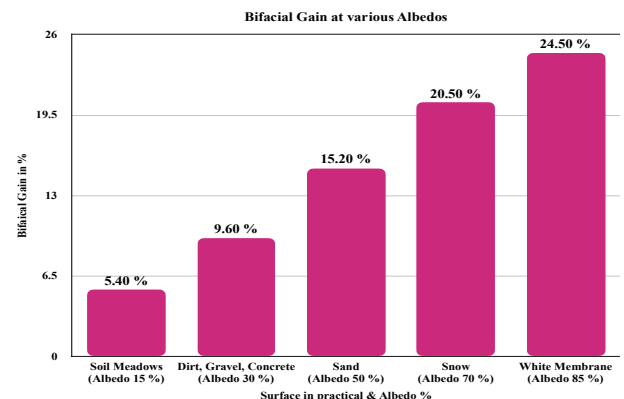


**Figure 6.** Various Albedos Considered for Analysis



### 3. RESULTS AND DISCUSSIONS

In this paper reliability improvement methodology with hybrid IGBT is proposed for the PV inverter. The hybrid IGBT consists of Silicon (Si) IGBT and Silicon Carbide (SiC) Schottky diode. A test case of 3-kW Monofacial and Bifacial grid connected PV inverter system with various albedos is considered under the following cases

- PV Inverter Reliability Evaluation with Conventional IGBT
- PV Inverter Reliability Evaluation with Hybrid IGBT

#### 3.1. PV Inverter Reliability Evaluation with Conventional IGBT

In this case reliability evaluation of 3-kW Monofacial and Bifacial grid connected PV inverter system with various albedos is implemented with conventional IGBT. The yearly MP is translated into JT for different albedos using the foster electrothermal model shown in *figure. 7*. Since the JT follows an irregular profile, a counting algorithm is required to analyse it.

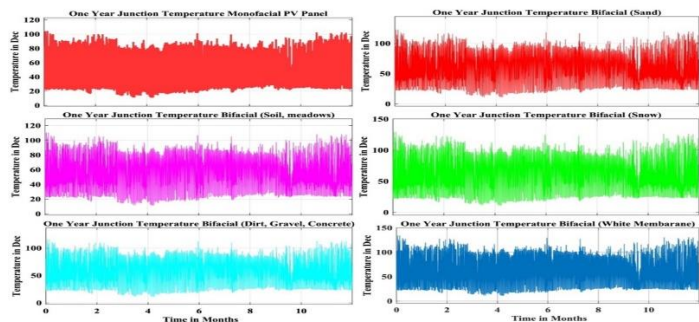
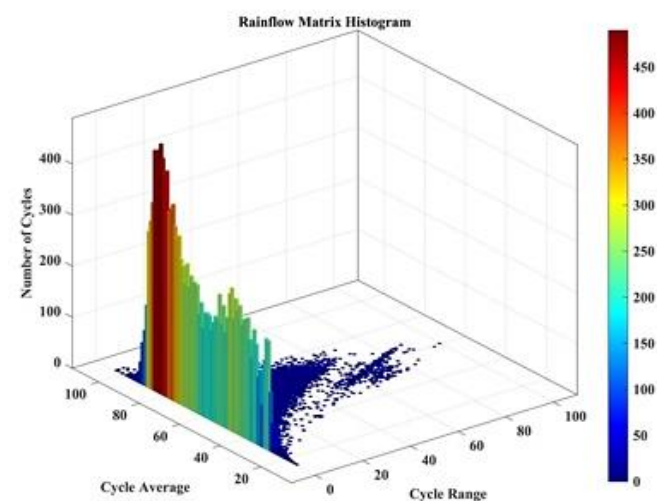
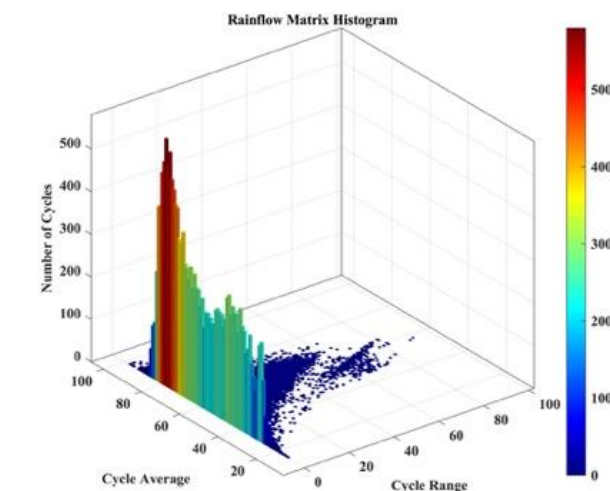


Figure. 7. Translated JT for Yearly Mission Profile with Conventional IGBT

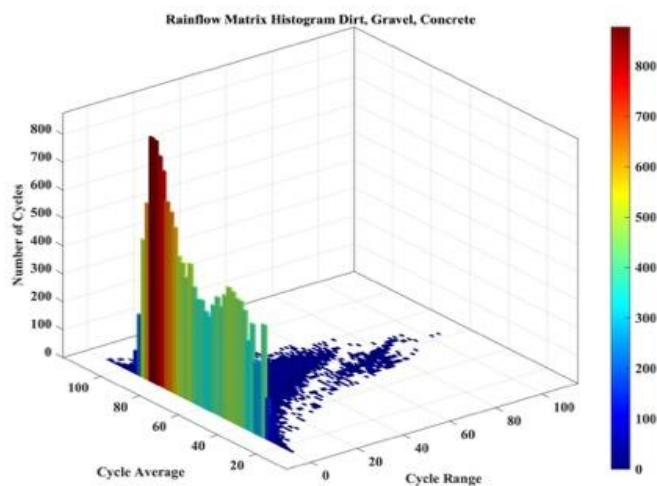
The Rainflow Counting (CRF) algorithm used to extract the thermal profiles JT for various albedos. It analyses the profiles by determining the number of cycles, average cycle count, and the cycle range as show in *figure. 8*.



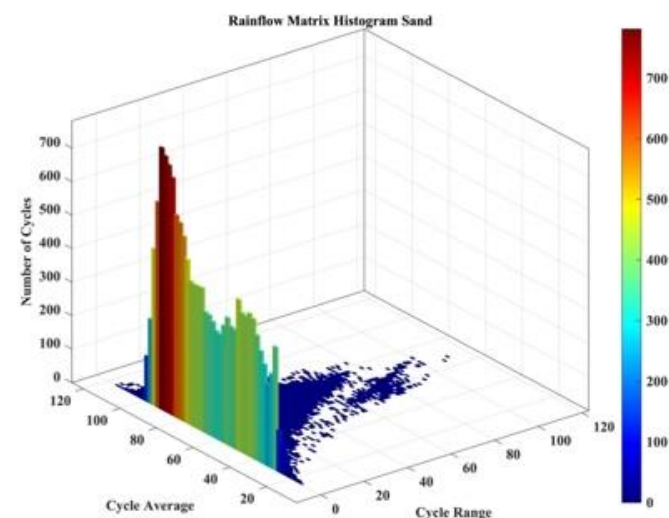
(a) Monofacial



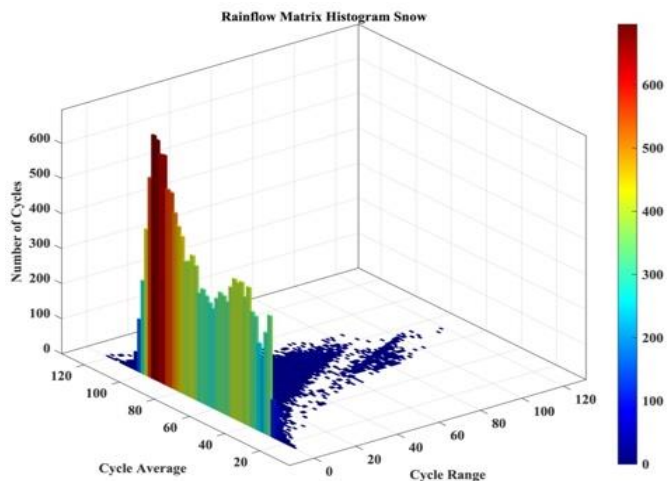
(b) Soil, Meadows



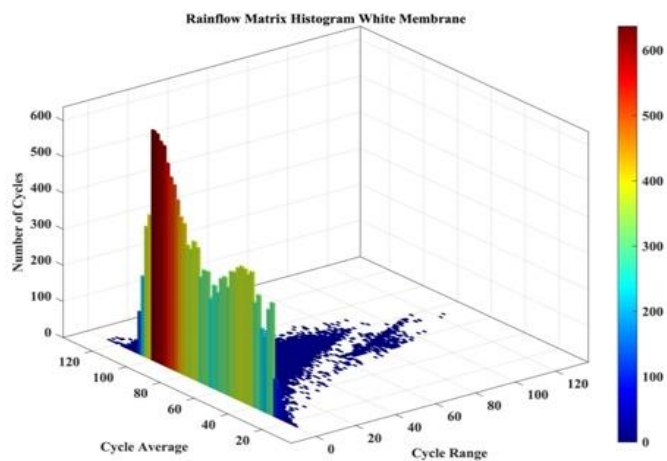
(c) Dirt, Gravel, Concrete



(d) Sand



(e) Snow



(f) White Membrane

**Figure 8.** CRF algorithm for various Albedos with Conventional IGBT

The LMCS algorithm is utilized to produce a population of 10,000 and LF is calculated at each population using *equation. 1*. The calculated LF at each population is then fitted in the Weibull distribution as shown in *figure. 9*.

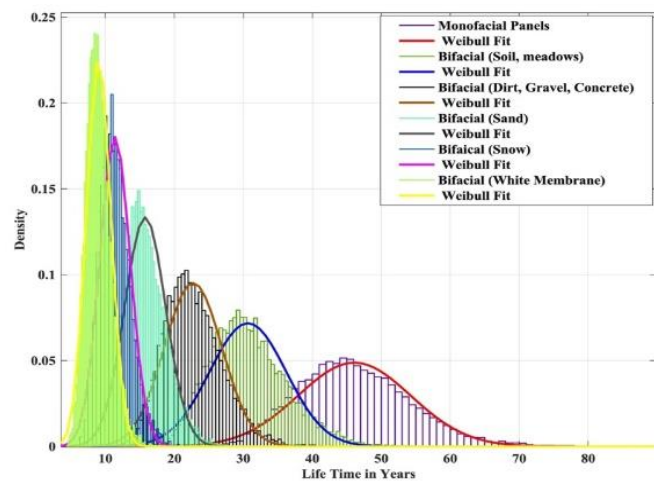


**Figure 9.** LMCS and Weibull Distribution with Conventional IGBT

From the Weibull distribution the scale and shape parameters are evaluated and reliability function at LC is calculated using *equation. 2*, LS is calculated using *equation. 3*. The LC for monofacial and bifacial panel are shown in *figure. 10* and *figure. 11* respectively.

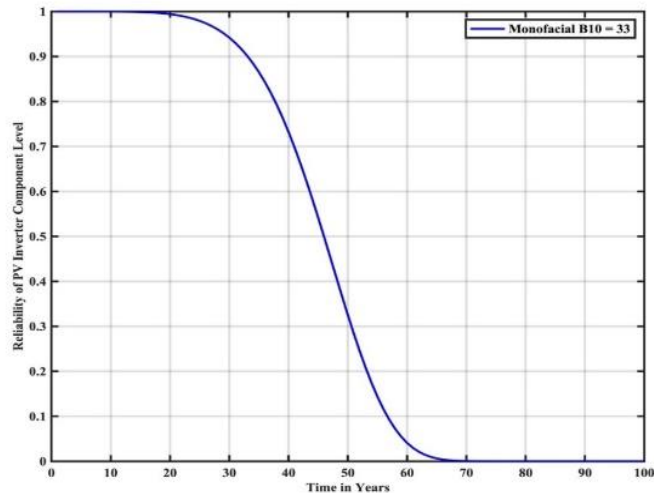


**Figure 10.** LC R(t) for Monofacial Panel with Conventional IGBT

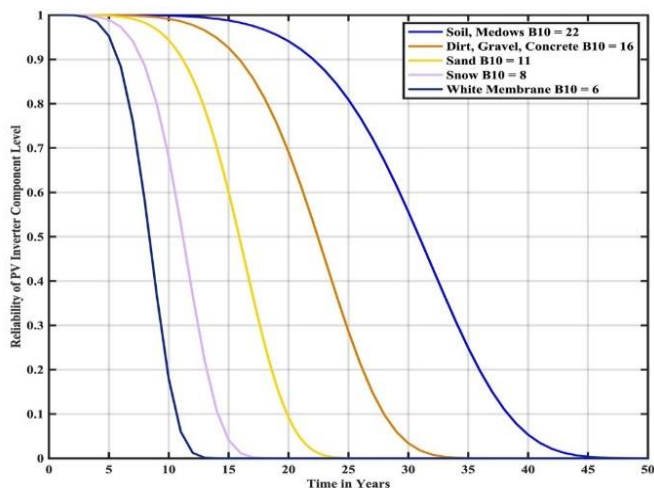


**Figure 11.** LC R(t) for Bifacial Panel with Conventional IGBT

In *figure. 10* and *figure. 11*, B10 lifeline ( $R(t)=0.9$ ) intersects the LC reliability curve for monofacial and bifacial with various albedos are tabulated in *table 2*.

**Table 2. B10 lifetime at LC with Conventional IGBT**

S. No.	Type of the Panel	B10 Lifetime in Years
1	Monofacial	33
2	Bifacial-Soil Meadows (Albedo 15 %)	22
3	Bifacial-Dirt, Gravel, Concrete (Albedo 30 %)	16
4	Bifacial-Sand (Albedo 50 %)	11
5	Bifacial-Snow (Albedo 70 %)	8
6	Bifacial-White Membrane (Albedo 85 %)	6

The LS for monofacial and bifacial panel are shown in *figure. 12* and *figure. 13* respectively.

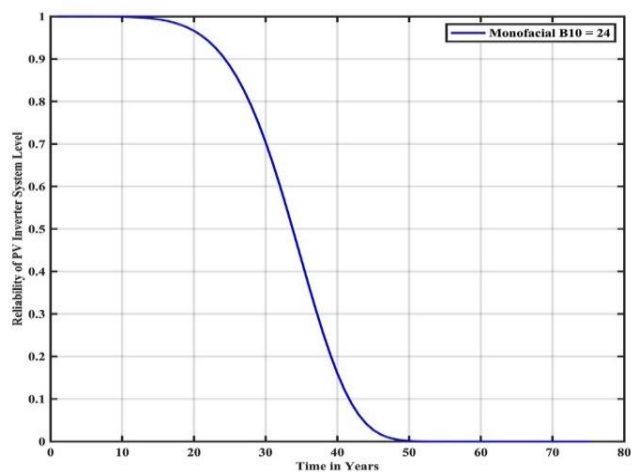


**Figure 12.** LS R(t) for Monofacial Panel with Conventional IGBT

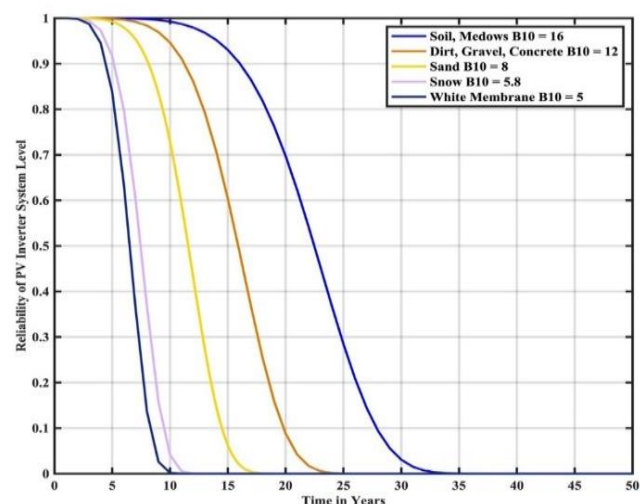


**Figure 13.** LS R(t) for Bifacial Panel with Conventional IGBT

In *figure. 12* and *figure. 13*, B10 lifeline ( $R(t)=0.9$ ) intersects the LS reliability curve for monofacial and bifacial with various albedos are tabulated in *table 3*.

**Table 3. B10 lifetime at LS with Conventional IGBT**

S. No.	Type of the Panel	B10 Lifetime in Years
1	Monofacial	24
2	Bifacial-Soil Meadows (Albedo 15 %)	16
3	Bifacial-Dirt, Gravel, Concrete (Albedo 30 %)	12
4	Bifacial-Sand (Albedo 50 %)	8
5	Bifacial-Snow (Albedo 70 %)	5.8
6	Bifacial-White Membrane (Albedo 85 %)	5

In both cases the decreasing trend is observed in B10 lifetime with the increase in Albedo. Hence reliability improvement methodology is needed.

### 3.2. PV Inverter Reliability Evaluation with Hybrid IGBT

In this case reliability evaluation of 3-kW Monofacial and Bifacial grid connected PV inverter system with various albedos is implemented with hybrid IGBT (Si-IGBT with SiC-Diode). The yearly MP is translated into JT for different albedos using the foster electrothermal model shown in *figure. 14*. Since the JT follows an irregular profile, a counting algorithm is required to analyse it.

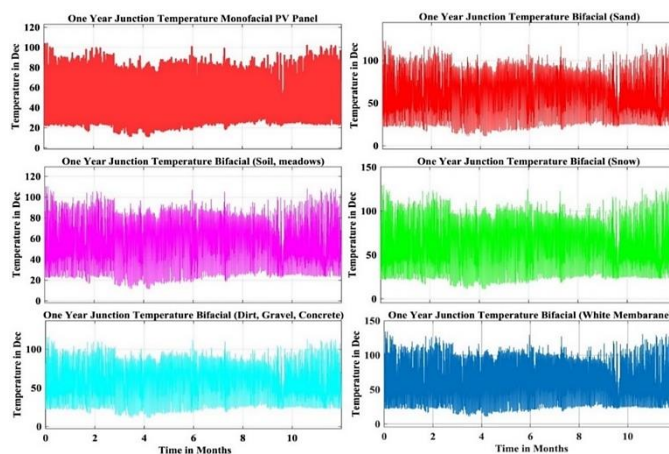
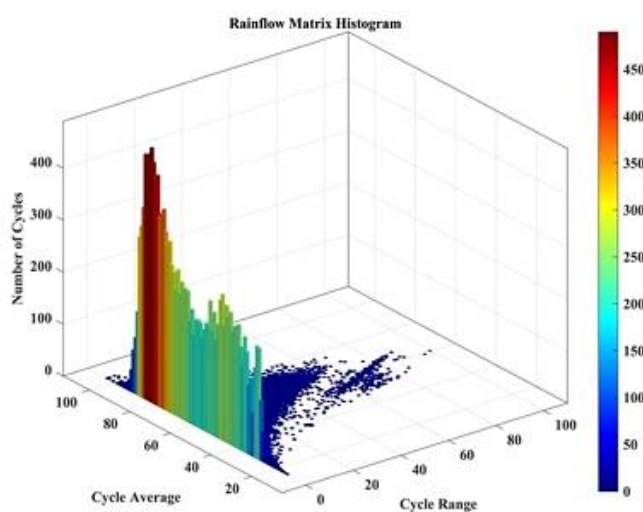


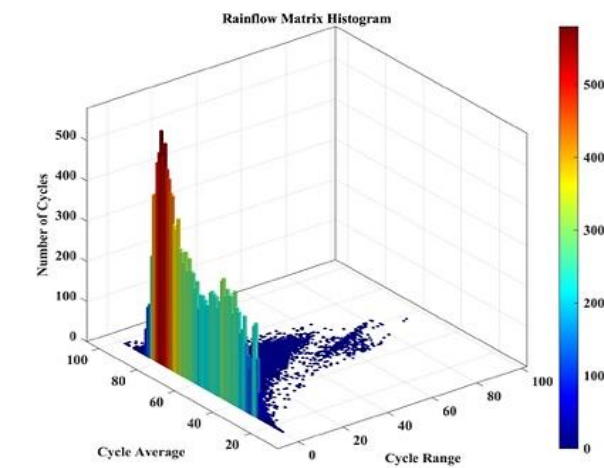
**Figure 14.** Translated JT for Yearly Mission Profile with Hybrid IGBT

The Rainflow Counting (CRF) algorithm used to extract the thermal profiles JT for various albedos. It analyses the profiles by determining the number of cycles, average cycle count, and the cycle range as show in *figure. 15*.

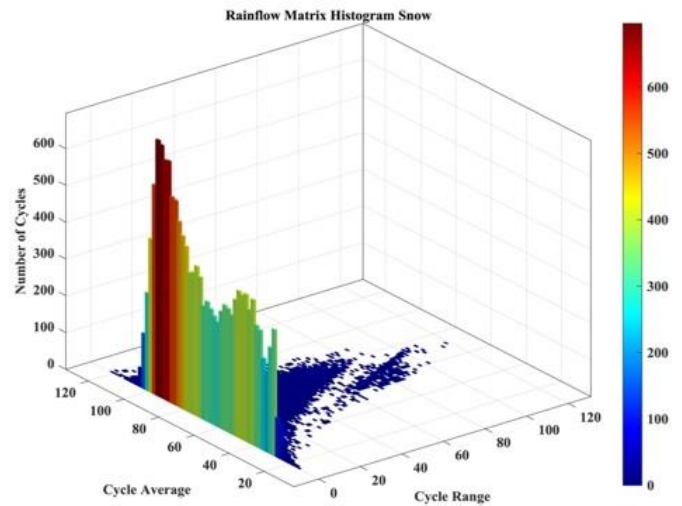


(a) Monofacial

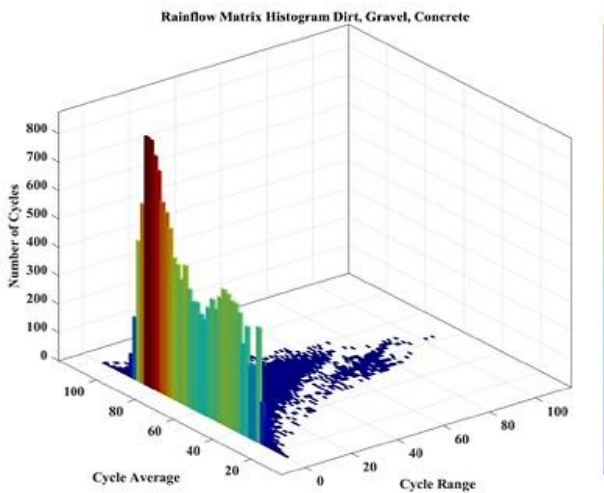




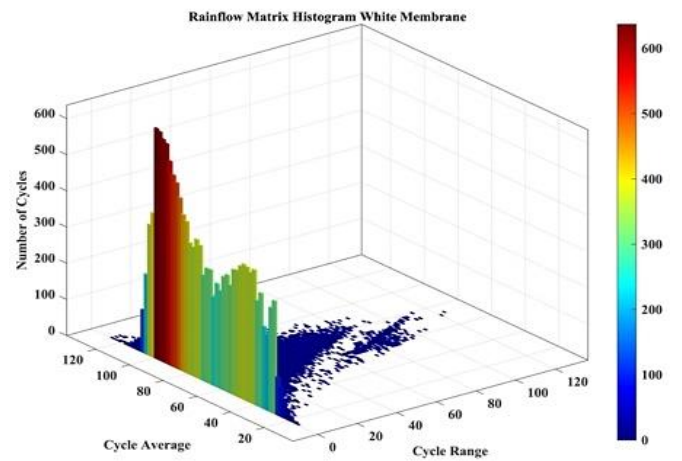
(b) Soil, Meadows



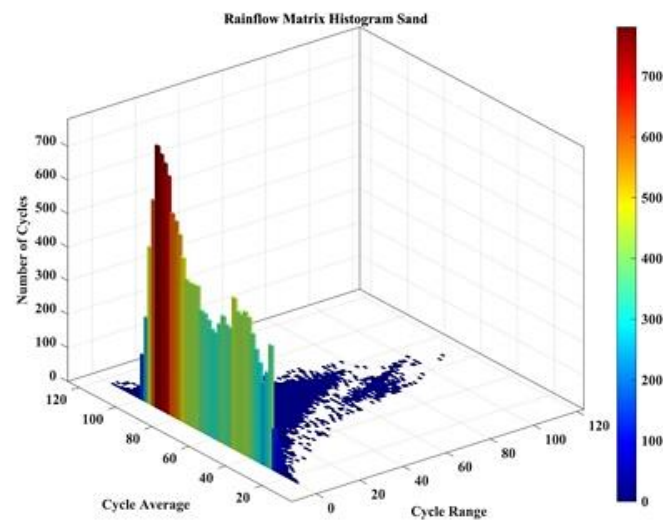
(e) Snow



(c) Dirt, Gravel, Concrete



(f) White Membrane



(d) Sand

**Figure. 15** CRF algorithm for various Albedos with Hybrid IGBT

The LMCS algorithm is utilized to produce a population of 10,000 and LF is calculated at each population using *equation. 1*. The calculated LF at each population is then fitted in the Weibull distribution as shown in *figure. 16*.

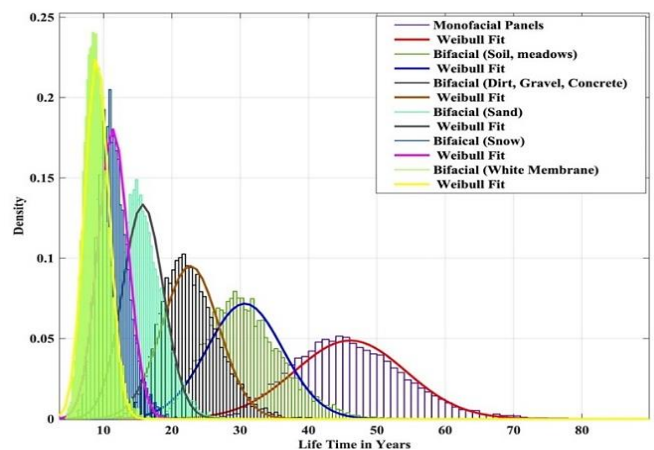


**Figure. 16** LMCS and Weibull Distribution with Hybrid IGBT

From the Weibull distribution the scale and shape parameters are evaluated and reliability function at LC is calculated using equation. 2, LS is calculated using equation. 3. The LC for monofacial and bifacial panel are shown in figure. 17 and figure. 18 respectively.

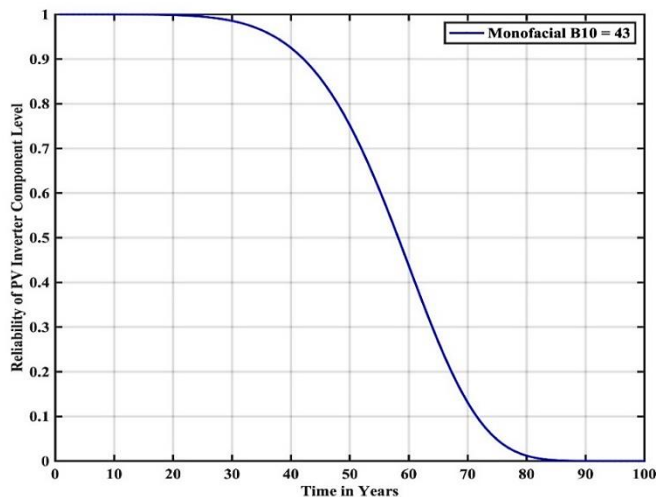


**Figure. 17** LC R(t) for Monofacial Panel with Hybrid IGBT

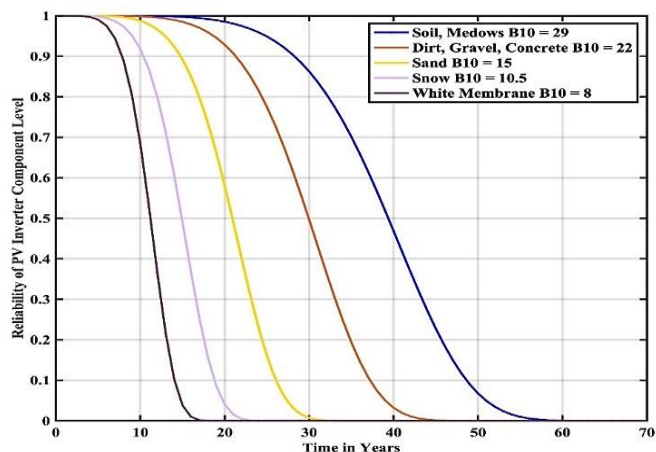


**Figure. 18** LC R(t) for Bifacial Panel with Hybrid IGBT

In figure. 17 and figure. 18, B10 lifeline ( $R(t)=0.9$ ) intersects the LC reliability curve for monofacial and bifacial with various albedos are tabulated in table 4.

**Table 4. B10 lifetime at LC with Hybrid IGBT**

S. No.	Type of the Panel	B10 Lifetime in Years
1	Monofacial	43
2	Bifacial-Soil Meadows (Albedo 15 %)	29
3	Bifacial-Dirt, Gravel, Concrete (Albedo 30 %)	22
4	Bifacial-Sand (Albedo 50 %)	15
5	Bifacial-Snow (Albedo 70 %)	10.5
6	Bifacial-White Membrane (Albedo 85 %)	8

The LS for monofacial and bifacial panel are shown in figure. 19 and figure 20 respectively.

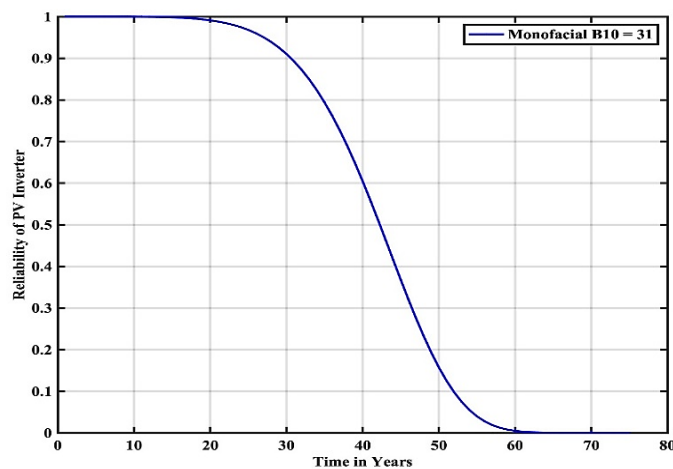


**Figure. 19** LS R(t) for Monofacial Panel with Hybrid IGBT

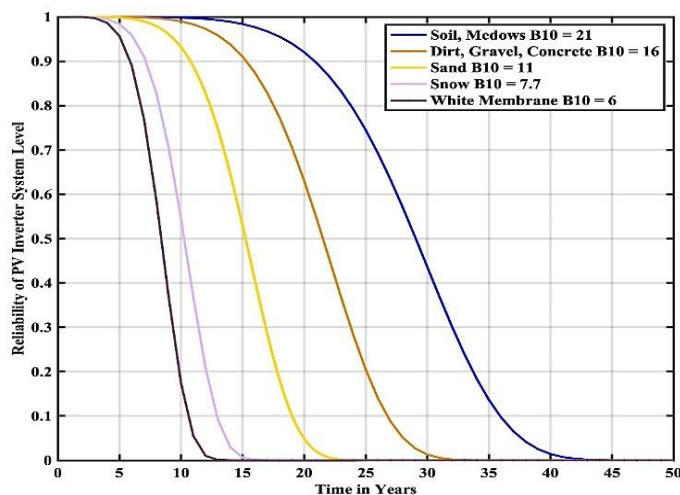


**Figure. 20** LS R(t) for Bifacial Panel with Hybrid IGBT

In figure. 19 and figure. 20, B10 lifeline ( $R(t)=0.9$ ) intersects the LS reliability curve for monofacial and bifacial with various albedos are tabulated in table 5.

**Table 5. B10 lifetime at LS with Hybrid IGBT**

S.No.	Type of the Panel	B10 Lifetime in Years
1	Monofacial	31
2	Bifacial-Soil Meadows (Albedo 15 %)	21
3	Bifacial-Dirt, Gravel, Concrete (Albedo 30 %)	16
4	Bifacial-Sand (Albedo 50 %)	11
5	Bifacial-Snow (Albedo 70 %)	7.7
6	Bifacial-White Membrane (Albedo 85 %)	6



With the proposed Hybrid IGBT the B10 lifetime is improved at all the cases.

#### 4. COMPARISON ANALYSIS

The reliability performance of proposed hybrid IGBT is compared with the conventional IGBT. The LC B10 lifetime comparison is presented in *figure. 21* and the LS B10 lifetime comparison is presented in *figure. 22*. In both the cases the proposed Hybrid IGBT significantly improves the reliability i.e., B10 lifetime.

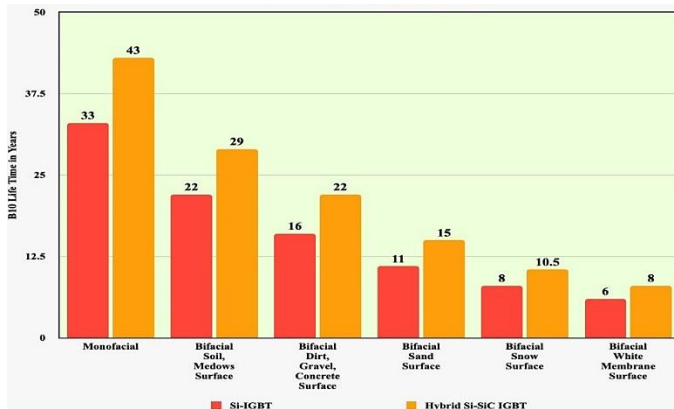


Figure 21. LC B10 lifetime comparison

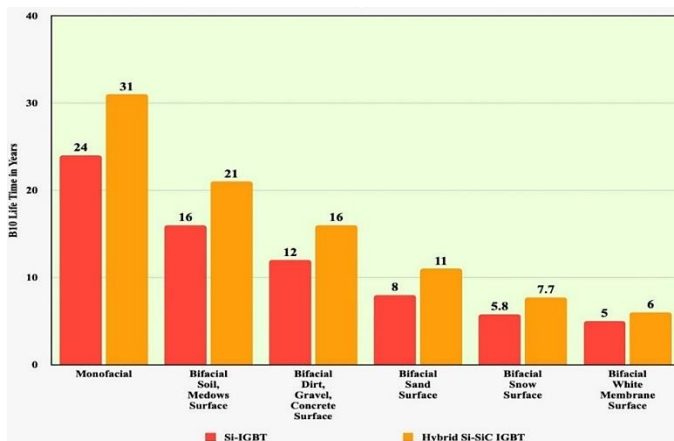


Figure 22. LS B10 lifetime comparison

#### 5. CONCLUSION

In this paper reliability improvement methodology with hybrid IGBT is proposed for the PV inverter. The hybrid IGBT consists of Silicon (Si) IGBT and Silicon Carbide (SiC) Schottky diode. A test case of 3-kW Monofacial and Bifacial grid connected PV inverter system with various albedos is considered. Mission profile for one year at Hyderabad, India location is logged for the assessment. Foster ETM is used to obtain the junction temperature (JT). JT variations are analyzed by using Rainflow (CRF) algorithm. Monte Carlo Simulation (LMCS) is used to produce 10000 populations. B10 lifetime is calculated for the proposed hybrid IGBT. The effectiveness of the proposed hybrid IGBT is evaluated in comparison with conventional IGBT. In bifacial case decreasing trend is observed in B10 lifetime with the increase in Albedo. Hence reliability

improvement methodology is needed, with the proposed hybrid IGBT significantly improves the reliability performance of the PV inverter in all the cases.

#### REFERENCES

- [1] M. Vimala, G. Ramadas, M. Perarasi, A. M. Manokar, and R. Sathyamurthy, "A Review of Different Types of Solar Cell Materials Employed in Bifacial Solar Photovoltaic Panel," *Energies*, vol. 16, no. 8, 2023, doi: 10.3390/en16083605.
- [2] J. Johnson and S. Manikandan, "Experimental study and model development of bifacial photovoltaic power plants for Indian climatic zones," *Energy*, vol. 284, 2023, doi: 10.1016/j.energy.2023.128693.
- [3] M. Mustapha et al., "Mathematical modeling and experimental validation of bifacial photovoltaic-thermal system with mirror reflector," *Case Stud. Therm. Eng.*, vol. 43, 2023, doi: 10.1016/j.csite.2023.102800.
- [4] C. Bai and M. Kim, "Single Power-Conversion Active-Clamped AC/DC Converter Employing Si/SiC Hybrid Switch," *IEEE Trans. Ind. Electron.*, vol. 71, no. 2, 2024, doi: 10.1109/TIE.2023.3262889.
- [5] X. Deng et al., "A Hybrid-Channel Injection Enhanced Modulation 4H-SiC IGBT Transistors with Improved Performance," *IEEE Trans. Electron Devices*, vol. 69, no. 8, 2022, doi: 10.1109/TED.2022.3183555.
- [6] H. Qin, S. Xie, Q. Xun, F. Zhang, Z. Xu, and L. Wang, "An optimized parameter design method of SiC/Si hybrid switch considering turn-off current spike," *Energy Reports*, vol. 8, 2022, doi: 10.1016/j.egy.2022.08.029.
- [7] Y. Wang, M. Chen, and D. Xu, "Design of Low Inductance SiC-MOS/Si-IGBT Hybrid Module for PV Inverters," *IEEE Open J. Power Electron.*, vol. 3, 2022, doi: 10.1109/OJPEL.2022.3224140.
- [8] T. Yin, L. Lin, C. Xu, D. Zhu, and K. Jing, "A Hybrid Modular Multilevel Converter Comprising SiC MOSFET and Si IGBT With Its Specialized Modulation and Voltage Balancing Scheme," *IEEE Trans. Ind. Electron.*, vol. 69, no. 11, 2022, doi: 10.1109/TIE.2021.3118372.
- [9] H. Liu, T. Zhao, and X. Wu, "Performance Evaluation of Si/SiC Hybrid Switch-Based Three-Level Active Neutral-Point-Clamped Inverter," *IEEE Open J. Ind. Appl.*, vol. 3, 2022, doi: 10.1109/OJIA.2022.3179225.
- [10] C. Liu et al., "Hybrid SiC-Si DC-AC Topology: SHEPWM Si-IGBT Master Unit Handling High Power Integrated with Partial-Power SiC-MOSFET Slave Unit Improving Performance," *IEEE Trans. Power Electron.*, vol. 37, no. 3, 2022, doi: 10.1109/TPEL.2021.3114322.
- [11] H. Liu, J. Zhou, T. Zhao, and X. Xu, "Si IGBT and SiC MOSFET Hybrid Switch-Based Solid State Circuit Breaker for DC Applications," in *2022 IEEE Energy Conversion Congress and Exposition, ECCE 2022*, 2022, doi: 10.1109/ECCE50734.2022.9948172.
- [12] L. Tan, P. Liu, C. She, P. Xu, L. Yan, and H. Quan, "Heat Dissipation Characteristics of IGBT Module Based on Flow-Solid Coupling," *Micromachines*, vol. 13, no. 4, 2022, doi: 10.3390/mi13040554.
- [13] Z. Zhu, C. Tu, B. Xiao, L. Long, F. Jiang, and S. Liu, "Research on Characteristics of SiC FET/Si IGBT and SiC MOSFET/Si IGBT Hybrid Switches," in *2022 4th International Conference on Smart Power and Internet Energy Systems, SPIES 2022*, 2022, doi: 10.1109/SPIES55999.2022.10082437.
- [14] Z. Li et al., "Dynamic Gate Delay Time Control of Si/SiC Hybrid Switch for Loss Minimization in Voltage Source Inverter," *IEEE J. Emerg. Sel. Top. Power Electron.*, vol. 10, no. 4, 2022, doi: 10.1109/JESTPE.2021.3137332.
- [15] C. L. Kahraman, S. Lakshmeesha, S. Rosado, and T. Wijekoon, "Impact of forward recovery effects in different Si-IGBT technologies used in hybrid Si-IGBT, SiC-MOSFET based ANPC topology," in *Conference Proceedings - IEEE Applied Power Electronics Conference and Exposition - APEC*, 2022, doi: 10.1109/APEC43599.2022.9773782.
- [16] A. Deshpande, R. Paul, A. Imran Emon, Z. Yuan, H. Peng, and F. Luo, "Si-IGBT and SiC-MOSFET hybrid switch-based 1.7 kV half-bridge power

module,” *Power Electron. Devices Components*, vol. 3, 2022, doi: 10.1016/j.pedc.2022.100020.

[17] D. Woldegiorgis and H. A. Mantooth, “Precise Electro-thermal Power Loss Model of a Three-level ANPC Inverter with Hybrid Si/SiC Switches,” *Chinese J. Electr. Eng.*, vol. 8, no. 3, 2022, doi: 10.23919/CJEE.2022.000027.

[18] K. Jing, L. Lin, T. Yin, and Q. Huang, “Flying-capacitor MMC Topology Combining Si IGBT and SiC MOSFET with Its Modulation Strategy,” *Gaodianya Jishu/High Volt. Eng.*, vol. 48, no. 10, 2022, doi: 10.13336/j.1003-6520.hve.20210777.

[19] H. Liu, T. Zhao, X. Xu, and J. Zhou, “Conduction Time Variation-Based Active Thermal Control Method for Si and SiC Hybrid Switch,” in *2022 IEEE Energy Conversion Congress and Exposition, ECCE 2022*, 2022, doi: 10.1109/ECCE50734.2022.9947678.

[20] F. Kayser, F. Pfirsch, F. J. Niedernostheide, R. Baburske, and H. G. Eckel, “Novel Si-SiC hybrid switch and its design optimization path,” in *Proceedings of the International Symposium on Power Semiconductor Devices and ICs*, 2022, vol. 2022-May, doi: 10.1109/ISPSD49238.2022.9813676.

[21] Y. Ding et al., “Degradation of Si/SiC Hybrid Switch under AC power cycle,” in *Conference Proceedings - IEEE Applied Power Electronics Conference and Exposition - APEC*, 2022, doi: 10.1109/APEC43599.2022.9773458.

[22] D. Yıldırım, M. H. Akşit, I. Çadırcı, and M. Ermiş, “All-SiC Traction Converter for Light Rail Transportation Systems: Design Methodology and Development of 165 kVA Prototype,” *Electron.*, vol. 11, no. 9, 2022, doi: 10.3390/electronics11091438.

[23] S. Wang, Z. Xia, H. Duan, C. Ma, S. Lu, and S. Li, “A Si IGBT and SiC MOSFET Hybrid Full-Bridge Inverter and Its Modulation Scheme,” in *2022 International Conference on Electrical Machines and Systems, ICEMS 2022*, 2022, doi: 10.1109/ICEMS56177.2022.9983311.

[24] N. Rigogiannis, A. Kotsidimou, I. Arzanas, C. Kyritsi, and N. Papanikolaou, “Comparative Performance Study of Hybrid Si/SiC Insulated-Gate Bipolar Transistors,” in *2022 IEEE 7th Forum on Research and Technologies for Society and Industry Innovation, RTSI 2022*, 2022, doi: 10.1109/RTSI55261.2022.9905217.



© 2024 by the Srikanth S and Dr. Byamakesh Nayak publication under the terms and conditions of the Creative Commons Attribution (CC BY) license

(<http://creativecommons.org/licenses/by/4.0/>).